Cardiology in the Young (2014), **24**, 661–674
doi:10.1017/S1047951113000978

Original Article

Left ventricular rotation and right–left ventricular interaction in congenital heart disease: the acute effects of interventional closure of patent arterial ducts and atrial septal defects*

Kai T. Laser,[1] Nikolaus A. Haas,[1] Markus Fischer,[1] Sheeraz Habash,[1] Franziska Degener,[1] Christian Prinz,[1] Hermann Körperich,[2] Eugen Sandica,[1] Deniz Kececioglu[1]

[1]*Center for Congenital Heart Defects;* [2]*Institute for Radiology, Nuclear Medicine and Molecular Imaging, Heart and Diabetes Center Northrhine-Westfalia, Ruhr-University of Bochum, Bad Oeynhausen, Germany*

Abstract *Background:* Left ventricular rotation is physiologically affected by acute changes in preload. We investigated the acute effect of preload changes in chronically underloaded and overloaded left ventricles in children with shunt lesions. *Methods:* A total of 15 patients with atrial septal defects (Group A: 7.4 ± 4.7 years, 11 females) and 14 patients with patent arterial ducts (Group B: 2.7 ± 3.1 years, 10 females) were investigated using 2D speckle-tracking echocardiography before and after interventional catheterisation. The rotational parameters of the patient group were compared with those of 29 matched healthy children (Group C). *Results:* Maximal torsion (A: 2.45 ± 0.9°/cm versus C: 1.8 ± 0.8°/cm, $p < 0.05$), apical peak systolic rotation (A: 12.6 ± 5.7° versus C: 8.7 ± 3.5°, $p < 0.05$), and the peak diastolic torsion rate (A: −147 ± 48°/second versus C: −110 ± 31°/second, $p < 0.05$) were elevated in Group A and dropped immediately to normal values after intervention (maximal torsion 1.5 ± 1.1°/cm, $p < 0.05$, apical peak systolic rotation 7.2 ± 4.1°, $p < 0.05$, and peak diastolic torsion rate −106 ± 35°/second, $p < 0.05$). Patients in Group B had decreased maximal torsion (B: 1.8 ± 1.1°/cm versus C: 3.8 ± 1.4°/cm, $p < 0.05$) and apical peak systolic rotation (B: 8.3 ± 6.1° versus C: 13.9 ± 4.3°, $p < 0.05$). Defect closure was followed by an increase in maximal torsion (B: 2.7 ± 1.4°/cm, $p < 0.05$) and the peak diastolic torsion rate (B: −133 ± 66°/second versus −176 ± 84°/second, $p < 0.05$). *Conclusions:* Patients with chronically underloaded left ventricles compensate with an enhanced apical peak systolic rotation, maximal torsion, and quicker diastolic untwisting to facilitate diastolic filling. In patients with left ventricular dilatation by volume overload, the peak systolic apical rotation and the maximal torsion are decreased. After normalisation of the preload, they immediately return to normal and diastolic untwisting rebounds. These mechanisms are important for understanding the remodelling processes.

Keywords: Congenital heart disease; preload; echocardiography; shunt; torsion

Received: 28 December 2012; Accepted: 22 June 2013; First published online: 29 July 2013

FROM AN ANATOMICAL AND PHYSIOLOGICAL POINT of view, different forms of cardiac deformations exist during a cardiac cycle as a result of the interaction between muscle fibres. Systolic cardiac deformation results in longitudinal shortening from the base to the apex of both ventricles, radial thickening, circumferential shortening, and a twisting rotational component for the left ventricle.

Tissue Doppler provided the first insights into regional myocardial velocities as well as active deformation processes with high temporal and spatial resolutions.[1,2] The technique has been supplemented by 2D greyscale speckle-tracking imaging, which is not angle-dependent and provides much easier

*This paper was presented at Poster 45th Annual Meeting of the Association for European Paediatric Cardiology, May 18–21, 2011 Granada, Spain; and Oral presentation 47th Annual meeting of the Japanese Society of Pediatric Cardiology and Cardiac Surgery, 2011 Fukuoka, Japan

Correspondence to: K. T. Laser, MD, Center for Congenital Heart Defects, Heart and Diabetes Center, Northrhine-Westfalia, Ruhr-University of Bochum, Georgstr 11, D-32545 Bad Oeynhausen, Germany. Tel: +49 (0)5731 97 3637; Fax: +49 (0)5731 97 2131; E-mail: tlaser@hdz-nrw.de

and less time-consuming post-processing of data. This is at the expense of a lower temporal resolution, vendor-dependent values, and, in part, reduced reproducibility because of the off-plane motion of speckles.[3,4]

Recently, the rotational component of left ventricular deformation has gained the interest of many working groups.[5] If the base and the apex of normal hearts are regarded from below the apex during systole, the base rotates clockwise and the apex rotates counterclockwise. The terms most often used for this pattern of deformation are "twist" and "torsion". Whereas the term "twist" is often simply used to express "wringing", torsion is defined as the instantaneous base-to-apex gradient of the rotation angle along the long axis of the left ventricle. The left ventricular maximal torsion reflects the greatest systolic angular displacement between apical counterclockwise and basal clockwise rotations.

Rotation can be measured by speckle tracking with comparable results to cardiovascular magnetic resonance imaging tagging, sonomicrometry, and tissue Doppler.[6–9] In general, it is believed to be a sensitive and age-dependent indicator of systolic and diastolic performance and myocardial molecular properties.[10] The loading conditions seem to influence the rotational parameters more than other parameters of deformation, with a higher effect of preload compared with afterload.[11–13] It has been shown that saline infusion in healthy individuals as a modification of preload results in an increase in maximal torsion.[14]

Clinically, elevation of the right ventricular preload in atrial septal defects is followed by dilatation of the right atrium and ventricle, whereas an elevation in the left ventricular preload in patent arterial ducts is followed by dilatation of the left atrium and ventricle due to an increased end-diastolic volume. Further, these chambers show an increased output and distensibility.[15] In children, closure of shunts results in recompensation of first the systolic and then the diastolic left ventricular function within a few months.[16] In patients with atrial septal defects, the left ventricle is smaller than normal and has an atypical shape and decreased output because of pathological interventricular interactions with atypical septal shifting. This can result in diastolic dysfunction after shunt closure, especially in elderly patients.[17] Adults with patent arterial ducts also have less recompensatory forces, resulting in reduced ejection fractions many months after intervention.[18] There are very scarce data on acute rotational left ventricular mechanics after interventional therapy for shunt lesions. We tested the hypothesis of whether left ventricular torsion and untwisting are altered in patients with atrial septal defects and patent arterial ducts when the loading conditions change acutely after interventional therapy.

Methods

Study population

The study was performed between June 2007 and February 2011. We prospectively enrolled patients with atrial septal defect and patent arterial duct suitable for interventional therapy. Patients with a poor echocardiographic window and those with additional cardiac defects were pre-excluded. Written informed consent from parents, legal guardians, or caretakers was obtained for cardiac catheterisation on a routine basis. Cardiac catheterisation was carried out using deep conscious sedation and spontaneous breathing; echocardiographic assessment before and after intervention was performed on a routine basis. The study was reviewed and approved by the institutional ethics committee. A total of 29 patients were enrolled: 15 presented with an atrial septal defect and 14 presented with a patent arterial duct.

Atrial septal defect

The patients were referred for interventional closure because of transthoracal echocardiographic evidence on the haemodynamic relevance of the shunt and because of right ventricular dilatation. The demographic data of the patient and control groups are provided in Table 1; the haemodynamic and echocardiographic data are provided in Tables 2 and 3. Transoesophageal echocardiography was performed to rule out partial anomalous pulmonary venous drainage, for defect sizing during balloon interrogation, and to assess device localisation before release. As a routine institutional procedure, no shunt quantification was performed. The devices used for closure were six Amplatzer atrial septal defect occluders, four Biostar occluders, four Occlutec occluders, and one Cardia occluder. The defect size was assessed by balloon interrogation in all patients (range 10–24 mm).

Patent arterial duct

In patients with patent arterial ducts, interventional therapy was indicated based on left atrial and left ventricular dilatation. The systolic function was preserved in all patients. The demographic data of the patient and control groups are provided in Table 7; the haemodynamic echocardiographic data are provided in Tables 8 and 9. The devices used for closure were six Amplatzer duct occluders, four Nit occluders, and four Cook coils.

https://doi.org/10.1017/S1047951113000978 Published online by Cambridge University Press

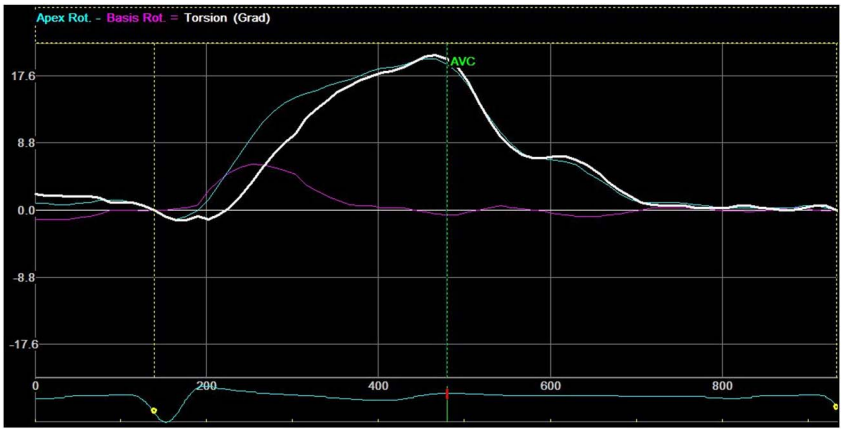

Figure 1.
Averaged rotational curves at the mitral valve (purple line) and apical (blue line) level. Torsion = apical rotation–basal rotation (white line). The systolic peak of the torsion curve represents maximal torsion.

Control group

Owing to the reported age-dependence of maximal torsion,[19] 29 age-matched, body surface area-matched, and sex-matched healthy children were included as controls (Tables 1 and 7). They were recruited as healthy volunteers to collect echocardiographic reference values. Similar to the patient protocol, the controls underwent standard echocardiographic evaluations to exclude structural cardiac diseases.

Echocardiographic data acquisition

A Vivid 7® ultrasound machine (GE Medical Systems, Milwaukee, Wisconsin, United States of America) with 7S, 5S, and M3S probes (range 3–7 MHz), frame rates ranging from 55 to 90 frames/second, and second harmonic imaging was used. All patients were examined in a supine left lateral position. Clinical standard echocardiography included the measurement of left ventricular volumes and ejection fractions using biplane Simpson's method.

For speckle-tracking analysis, we scanned the left ventricular short-axis loops at apical, papillary muscle, and basal levels. Specific attention was paid to the cross-sections, making them as circular as possible. At the mitral valve level, atrial tissue was carefully excluded. To obtain a proper view of the apical rotation, exclusion of papillary muscles and the lowest slice with a persisting lumen was mandatory. In most cases, we were able to achieve this view from one to two intercostal spaces below the standard short-axis views. In addition, one four-chamber view was recorded and the longitudinal septal deformation was investigated. End-expiratory breath-hold was performed only if image quality was limited. Aortic and mitral valve Doppler signals were used to establish timing events in combination with electrocardiographic triggering. All examinations were performed by the same investigator. Data acquisition was performed one day before treatment and at 4–6 hours after intervention. Subsequent data analysis was performed on a personal computer workstation with the Echopac-Software (Version 6.1.2, GE Medical Systems) by an independent investigator in a blinded manner.

Left ventricular rotational values

Angular displacement of the left ventricle was determined by use of the 2D-Strain software at the apical and mitral valve level and has been referred to as rotation (°) in this article. Briefly, it calculates mean rotational values from all six segments that were used to calculate peak systolic apical, basal rotation, and maximal torsions (Fig 1). This was defined as the maximum instantaneous net difference in values between the apex and base of the left ventricle and was secondarily normalised to the left ventricular length, that is, maximal torsion (°/cm) = (apical rotation − basal rotation)/left ventricular diastolic longitudinal length.[19] In addition, the mean peak systolic and diastolic torsion rates were extracted from the apical and basal rotation velocity curves that were generated in the same way as described for maximal torsion (Fig 2).

Statistics

For data analysis, a two-tailed Student's t-test for unpaired data and a Student's t-test for paired data were applied when appropriate, considering $p < 0.05$ as being statistically significant. Normal distribution of the data was tested using the Kolmogorov–Smirnov test. A normal distribution was considered if the p-values were above 0.05. The

https://doi.org/10.1017/S1047951113000978 Published online by Cambridge University Press

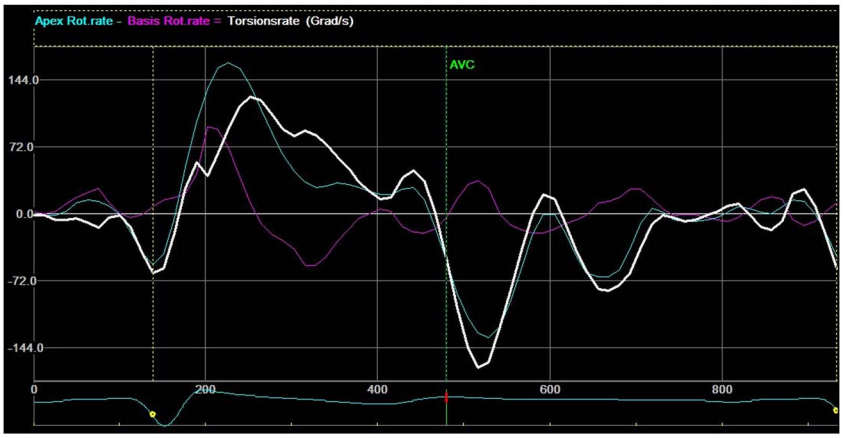

Figure 2.
Averaged rotation rate curves at the mitral valve (purple line) and apical (blue line) level. Torsion rate = basal–apical rotation rate. Maximal and minimal values of the torsion rate curve represent the peak systolic and diastolic torsion rates.

results are expressed as mean ± standard deviation. The statistical software package SPSS version 14 (Chicago, Illinois, United States of America) was used to perform the analysis. The intra-observer and inter-observer variabilities have been assessed in a previous study[20] and thus were not re-evaluated because of good comparability with other studies.[8]

Results

Demographic data

There were no significant differences in number, sex, age, height, weight, and body surface area between the patient and control groups with respect to atrial septal defect and patent arterial duct (Tables 1 and 7).

Conventional echocardiographic haemodynamic data in patients with atrial septal defects

In the M-mode measurements, the right ventricular end-diastolic diameters were elevated before closure and the left ventricular end-diastolic and end-systolic diameters were smaller compared with those of healthy controls (Table 2). Echocardiographic shunt quantification before atrial septal defect closure revealed a mean Qp/Qs ranging from 1.5 to 3.7 (mean 2.3 ± 0.74).

Table 1. Patients with atrial septal defects – demographic data.

	Patients	Control
Number	15	15*
Sex (male, female)	4, 11	4, 11*
Age (years)	7.4 ± 4.7	7.4 ± 3.5*
Weight (kg)	27 ± 16.8	27 ± 14.9*
Height (cm)	126 ± 21.5	123 ± 19*
BSA (m^2)	0.94 ± 0.3	0.94 ± 0.3*

BSA = body surface area
*Statistically non-significant

After interventional therapy, the heart rate dropped (95 ± 15 bpm versus 89 ± 15 bpm, $p < 0.05$). The end-diastolic right ventricular diameter dropped significantly (23.1 ± 4.2 mm versus 17.7 ± 3.2 mm, $p < 0.05$) and the end-diastolic left ventricular diameter increased (33.2 ± 3.8 versus 35.4 ± 4.1 mm, $p < 0.05$) upon closure (Table 2). Similar results for the left ventricle were obtained using volumetric measurements (Table 3) with an increase in the end-diastolic volume (41.7 ± 14.4 versus 46.9 ± 14.7 ml, $p < 0.05$), stroke volume (24.7 ± 9 versus 30.4 ± 9.9 ml, $p < 0.05$), and cardiac index (2.51 ± 0.58 versus 2.89 ± 0.65 L/minute/m^2); however, the end-systolic volumes remained stable.

Rotational parameters in patients with atrial septal defects

Compared with normal controls, in patients with atrial septal defects we found an increased peak systolic apical rotation (12.6 ± 5.7 versus 8.7 ± 3.5°, $p < 0.05$) without a significant influence on maximal torsion (2.45 ± 0.87°/cm, ns, Table 4). The peak diastolic torsion rate was also seen to be elevated (−146.9 ± 47.9 versus −110.2 ± 31.4°/second, $p < 0.05$). After interventional atrial septal defect closure, there was a decrease in maximal torsion (2.45 ± 0.87 versus 1.55 ± 1.07 °/cm, $p < 0.05$, Fig 3), peak systolic apical rotation (12.6 ± 5.7 versus 7.2 ± 4.1°, $p < 0.05$, Fig 4), and the peak diastolic torsion rate (−146.9 ± 47.9 versus −106.2 ± 34.1°/cm, Fig 5); however, the peak systolic basal rotation and the peak systolic torsion rate remained stable.

https://doi.org/10.1017/S1047951113000978 Published online by Cambridge University Press

Table 2. Patients with atrial septal defects – standard M-mode echocardiographic measurements.

	RVDd (mm)	LVDd (mm)	LVDs (mm)	FS (%)
ASD patients				
Pre	23.1 ± 4.2	33.2 ± 3.8	19.4 ± 2.9	42 ± 7
Post	17.7 ± 3.2	35.4 ± 4.1	19.7 ± 2.7	44 ± 6
	($p < 0.05$)	($p < 0.05$)	($p = 0.675$)	($p = 0.261$)
Control	12.0 ± 3.1	37.7 ± 5.0	22.7 ± 2.9	40 ± 4
Pre	($p < 0.05$)	($p < 0.05$)	($p < 0.05$)	ns
Post	($p < 0.05$)	ns	($p < 0.05$)	($p < 0.05$)

ASD = atrial septal defect; FS = fractional shortening; LVDd = left ventricular end-diastolic diameter; LVDs = left ventricular end-systolic diameter; ns = statistically non-significant; post = after intervention; pre = before intervention; RVDd = right ventricular end-diastolic diameter
Differences between patient data determined using the paired t-test and patient and control group data compared using the unpaired t-test

Table 3. Patients with atrial septal defects – left ventricular volumetric measurements using biplanar Simpson's method.

ASD patients	LV-EDV (ml)	LV-ESV (ml)	LV-SV (ml)	CI/BSA (L/minute/m^2)	heart rate (bpm)
Pre	41.7 ± 14.3	17.0 ± 5.8	24.7 ± 9.0	2.51 ± 0.58	95 ± 15
Post	46.9 ± 14.7	16.5 ± 5.5	30.4 ± 9.9	2.89 ± 0.65	89 ± 15
	($p < 0.05$)	ns	($p < 0.05$)	($p < 0.05$)	($p < 0.05$)

ASD = atrial septal defect; CI/BSA = cardiac index; normalised to body surface area; LV-EDV = left ventricular end-diastolic volume; LV-ESV = left ventricular end-systolic volume; LV-SV = left ventricular stroke volume; ns = statistically non-significant; post = after intervention; pre = before intervention
Results in mean ± SD
Differences between patient data

Table 4. Patients with atrial septal defects – rotational parameters of the left ventricle.

	Tor (°/cm)	Rot_{apex} (°)	Rot_{basis} (°)	$Torrate_{sys}$ (°/second)	$Torrate_{dia}$ (°/second)
ASD patients					
Pre	2.45 ± 0.87	12.6 ± 5.7	−5.5 ± 4.5	138.9 ± 48.5	−146.9 ± 47.9
Post	1.55 ± 1.07	7.2 ± 4.1	−4.6 ± 2.5	116.1 ± 40.5	−106.2 ± 34.1
	($p < 0.05$)	($p < 0.05$)	ns	ns	($p < 0.05$)
Control	1.85 ± 0.78	8.7 ± 3.5	−3.9 ± 2.3	114.8 ± 36.3	−110.2 ± 31.4
Pre	ns	($p < 0.05$)	ns	ns	($p < 0.05$)
Post	ns	ns	ns	ns	ns

ASD = atrial septal defect; ns = statistically non-significant; post = after intervention; pre = before intervention; Rot_{apex} = peak systolic apical rotation; Rot_{basis} = peak systolic basal rotation; Tor = maximal torsion; $Torrate_{dia}$ = peak diastolic torsion rate; $Torrate_{sys}$ = peak systolic torsion rate
Maximal and minimal values of the mean rotational curves of apical and basal short-axis loops and torsional parameters resulting from subtraction of the apical from the basal rotational curves
Results in mean ± SD
Differences between patient data using the paired t-test and patient and control group data compared using the unpaired t-test

Septal right-to-left ventricular interaction in patients with atrial septal defects

Compared with the control group, higher circumferential strain values were calculated at a global level in the short-axis loop of the left ventricle at the papillary muscle level (−20.64 ± 2.5% versus −16.75 ± 2.3%, $p < 0.05$, Table 5). In the segmental evaluation, this was evident for the anterior, anteroseptal, and lateral segments (Table 6). After atrial septal defect closure, these changes remained elevated in the anterior segment. In the apical four-chamber septal evaluation, a tendency towards higher longitudinal strain values at the basal level was observed. The systolic global circumferential strain rate values (−1.59 ± 0.25/second versus −1.21 ± 0.25/second, $p < 0.05$) and the diastolic longitudinal (2.10 ± 0.42/second versus 1.75 ± 0.41/second, $p < 0.05$) and circumferential (1.99 ± 0.46/second versus 1.47 ± 0.37/second, $p < 0.05$) strain rate values during peak E-wave were elevated before intervention. After atrial septal defect closure, only

https://doi.org/10.1017/S1047951113000978 Published online by Cambridge University Press

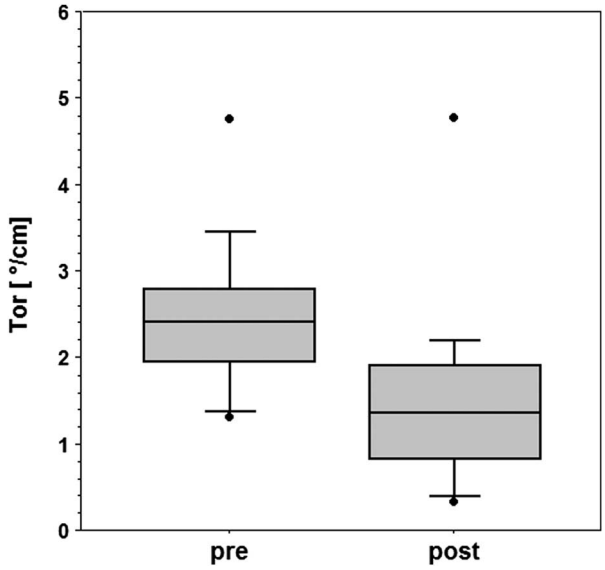

Figure 3.
Patients with atrial septal defects – maximal torsion before and after intervention.

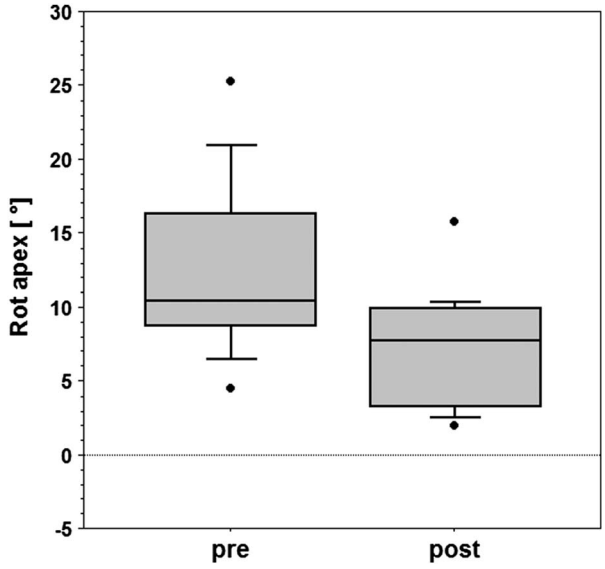

Figure 4.
Patients with atrial septal defects – peak systolic apical rotation before and after intervention.

the diastolic E-wave circumferential strain rate remained elevated, whereas intraindividual measurements resulted in a significant decrease in the circumferential strain rate (-1.37 ± 0.26/second, $p < 0.05$, Table 5).

Conventional echocardiographic haemodynamic data in patients with patent arterial ducts

Before shunt closure, the left ventricular end-diastolic (35.1 ± 4.3 versus 28.4 ± 7.3 mm, $p < 0.05$) and

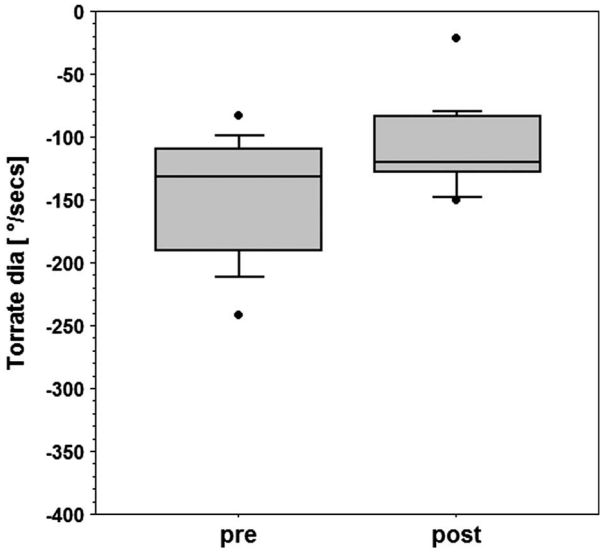

Figure 5.
Patients with atrial septal defects – peak diastolic torsion rate before and after intervention.

end-systolic diameters (20.2 ± 3.7 versus 15.9 ± 4.3 mm, $p < 0.05$) were increased in the M-mode measurements (Table 8). The right ventricular end-diastolic diameter and FS did not differ from those of the control group. The heart rate was not significantly different when compared with that of the control group (100 ± 23/minute).

After intervention, there was an increase in the right ventricular end-diastolic diameter (10.4 ± 2.6 mm versus 8.4 ± 2.0 mm, $p < 0.05$), whereas the left ventricular end-diastolic diameter (35.1 ± 4.3 versus 31.6 ± 4.3 mm, $p < 0.05$), fractional shortening ($43 \pm 5\%$ versus $39 \pm 6\%$, $p < 0.05$), and left atrial diameters (25.8 ± 4.4 versus 22.0 ± 4.4 mm) dropped. The volumetric measurements documented a decrease in the end-diastolic volume (37.3 ± 16.8 versus 27.2 ± 10.7 ml, $p < 0.05$), stroke volume (24.8 ± 9.1 versus 17.1 ± 7.1 ml, $p < 0.05$), and cardiac index (5.55 ± 1.98 versus 3.67 ± 1.84 L/minute/m^2, $p < 0.05$). The end-systolic volume and heart rate remained stable (Table 9).

Rotational parameters in patients with patent arterial ducts

In patients with patent arterial ducts, we found reduced maximal torsion (1.78 ± 1.11 versus 3.8 ± 1.4°/cm, $p < 0.05$) and peak systolic apical rotation (8.3 ± 6.1 versus 13.9 ± 4.3°, $p < 0.05$), whereas the peak systolic basal rotation, peak systolic torsion rate, and peak diastolic torsion rate were not significantly altered (Table 10).

https://doi.org/10.1017/S1047951113000978 Published online by Cambridge University Press

Table 5. Patients with atrial septal defects – global longitudinal and circumferential strain and strain rate values resulting from one apical four-chamber view including only the interventricular septum and one short-axis view at papillary muscle level before (pre) and after (post) intervention.

	GLS	GLSr	GLSr e	GLSr a	GCS	GCSr	GCSr e	GCSr a	GRS
ASD patients									
Pre	−22.01 ± 3.05	−1.43 ± 0.26	2.10 ± 0.42	1.10 ± 0.64	−20.64 ± 2.52	−1.59 ± 0.25	1.99 ± 0.46	0.63 ± 0.31	49.55 ± 18.60
Post	−22.61 ± 3.72	−1.47 ± 0.35	2.08 ± 0.63	0.91 ± 0.27	−20.40 ± 3.89	−1.37 ± 0.26	2.10 ± 0.57	0.53 ± 0.20	52.65 ± 17.34
	ns	ns	ns	ns	ns	($p < 0.05$)	ns	ns	ns
Control	−20.47 ± 2.29	−1.29 ± 0.18	1.75 ± 0.41	0.89 ± 0.30	−16.75 ± 2.27	−1.21 ± 0.25	1.47 ± 0.37	0.51 ± 0.26	46.49 ± 14.41
Pre	ns	ns	($p < 0.05$)	ns	($p < 0.05$)	($p < 0.05$)	($p < 0.05$)	ns	ns
Post	ns	ns	ns	ns	($p < 0.05$)	ns	($p < 0.05$)	ns	ns

ASD = atrial septal defect; ns = statistically non-significant

Values representing global strain/strain rate (GLS, GCS/GLSr, GCSr), peak diastolic strain rate at E-wave (GLSr e/GCSr e) and A-wave (GLSr a/GCSr a) timings

After shunt closure, there was an increase in maximal torsion (1.78 ± 1.11 versus 2.74 ± 1.45°/cm, Fig 6) and the peak diastolic torsion rate (−133.2 ± 66.0 versus −175.6 ± 83.9, $p < 0.05$, Fig 7). We did not observe any differences in peak systolic apical rotation (Fig 8) and peak systolic basal rotation but noticed a tendency towards a decrease in the systolic torsion rate. After intervention, the peak systolic apical rotation and peak systolic torsion rates were still significantly decreased.

Septal right-to-left ventricular interactions in patients with patent arterial ducts

Compared with the control group, higher circumferential strain values (−21.85 ± 3.76% versus −16.04 ± 3.91%, $p < 0.05$, Table 11) were calculated at a global level in the short-axis loop of the left ventricle at the papillary muscle level. In the segmental evaluation, this was evident for the inferior segment, and there was a comparable tendency towards not reaching significant values in the lateral, posterior, and septal segments (Table 12). After intervention, these values were no longer significantly elevated. The peak global longitudinal strain in the apical four-chamber septal evaluation was significantly higher in patients before intervention compared with controls (−20.7 ± 4.4% versus −16.5 ± 4.5%, $p < 0.05$, Table 11). At a segmental level, this was evident for the apical and middle segments; the deformation recovered after patent arterial duct closure. The systolic radial thickening was lower in the basal segments of the apical septal four-chamber view before and after intervention (Table 12). The diastolic global longitudinal E-wave strain rate was elevated previously but decreased after therapy (Table 11).

Discussion

It is a well-known physiologic phenomenon that cardiac loading conditions influence ventricular filling and performance. Especially in patients with shunt lesions, ventricular function can be maintained without causing clinical symptoms despite pulmonary hypercirculation and different effects on the preload. Left ventricular rotational deformation is one mechanism that can easily compensate acute changes in the preload in healthy individuals. We tested the hypothesis whether the same mechanisms can be applied to children with chronically volume-depleted or volume-overloaded ventricles, that is, those with atrial septal defects or patent arterial ducts, and examined the parameters shortly after interventional shunt closure and thereby preload changes.

The exact left ventricular anatomy is complex including helical and circumferential muscle fibre orientations. The basal two-thirds of the free left ventricular wall consist of three muscle layers. The subepicardial and subendocardial fibres run in different oblique angles, whereas the mid wall muscle fibres have a horizontal orientation. The apical part of the left ventricle lacks circumferential fibres and there is some uncertainty about the intraventricular septum. Helical subendocardial fibres run in a right-handed orientation with an average angle of about +60°, whereas subepicardial fibres run in a left-handed orientation with an average angle of about −50°.[21,22] There is still an ongoing debate on the mechanical interaction between muscle fibres. Of the theories, one states that there is an entire muscle band which in case of left ventricular acts as a double helix.[10,23,24] Other authors argue that there are regionally different amounts of muscle fibres working together with their fibrous matrix as a spatial netted mesh.[25] The impact of these anatomical and mechanical findings on rotational deformations in children with shunt lesions and acute changes in loading conditions were the major interests of this study.

https://doi.org/10.1017/S1047951113000978 Published online by Cambridge University Press

Table 6. Patients with atrial septal defects – segmental longitudinal (GLS), radial (GRS), and circumferential (GCS) strain values resulting from one apical four-chamber view including only the inter-ventricular septum, a basal, mid, and apical segment, and one short-axis view at the papillary muscle level including six segments (anterior, anteroseptal, inferior, lateral, posterior, and septal) before (pre) and after (post) intervention.

	Anterior	**Anteroseptal**	**Inferior**	**Lateral**	**Posterior**	**Septal**	**Apical**	**Basal**	**Mid**
ASD patients									
GCS pre	−28.53 ± 5.63	−29.11 ± 5.61	−15.74 ± 3.62	−18.32 ± 3.33	−10.21 ± 5.82	−24.32 ± 5.08			
GCS post	−24.48 ± 6.60	−27.15 ± 5.16	−18.53 ± 6.00	−17.85 ± 7.54	−11.64 ± 7.25	−26.37 ± 5.54			
	ns	ns	ns	ns	ns	ns			
GCS control	−16.61 ± 7.04	−23.70 ± 5.47	−16.79 ± 6.39	−11.14 ± 7.04	−10.52 ± 8.05	−23.44 ± 5.90			
Pre	($p < 0.05$)	($p < 0.05$)	ns	($p < 0.05$)	ns	ns			
Post	($p < 0.05$)	ns	ns	ns	ns	ns			
GRS pre	48.54 ± 16.64	43.43 ± 14.26	50.69 ± 22.64	54.21 ± 24.19	54.29 ± 26.07	45.80 ± 17.82	40.32 ± 3.56	38.83 ± 3.89	32.99 ± 3.56
GRS post	52.52 ± 19.48	48.12 ± 15.70	54.08 ± 21.40	54.99 ± 21.00	55.04 ± 21.51	48.86 ± 17.75	36.03 ± 4.94	52.41 ± 5.53	40.02 ± 4.89
	ns	ns	ns	ns	ns	ns	ns	ns	ns
GRS control	46.79 ± 18.99	41.02 ± 15.14	46.81 ± 18.50	52.73 ± 18.31	54.88 ± 17.88	36.74 ± 15.75	23.85 ± 2.81	36.64 ± 2.54	26.60 ± 2.33
Pre	ns	ns	ns	ns	ns	ns	ns	ns	ns
Post	ns	ns	ns	ns	ns	ns	ns	ns	ns
GLS pre							−22.44 ± 3.52	−21.60 ± 3.23	−21.98 ± 3.00
GLS post							−23.18 ± 4.26	−22.03 ± 4.22	−22.48 ± 3.89
							ns	ns	ns
GLS control							−20.93 ± 2.82	−19.45 ± 2.58	−20.47 ± 2.29
Pre							ns	ns	ns
Post							ns	ns	ns

ASD = atrial septal defect; ns = statistically non-significant

Values representing global segmental strain

Patients with atrial septal defects

The left ventricular end-diastolic diameters in patients with atrial septal defects were reduced when compared with those of the control group and returned to normal immediately after shunt closure. This is consistent with our hypothesis that in patients with atrial septal defects the left ventricle is "underfilled". Further, the stroke volume, heart rate, and cardiac index increased in the patient group after intervention and thereby volume loading. Before intervention, these patients with large right ventricles and underfilled left ventricles had higher peak systolic left ventricular circumferential strain values at the papillary muscle level, especially in the anterior, anteroseptal and lateral segments, as well as increased apical rotations when compared with the control group. This could not be proven for longitudinal and radial strain values and for maximal torsion. Further, the left ventricular systolic circumferential, diastolic longitudinal, and circumferential E-wave strain rates were elevated in patients with atrial septal defects. These changes mimic the influence of a right ventricular volume overload on the compensational cardiomechanics of the left ventricle affecting the systolic and diastolic deformations and the velocity of events. The regional segmental changes in circumferential deformation might affect apical counterclockwise rotation more than basal clockwise rotation. After atrial septal defect closure, the left ventricular circumferential deformation at the mid-ventricular anteroseptal and lateral levels was no longer elevated, compared with the control group, and the apical rotation decreased significantly in the intra-individual measurements, resulting in a significant decrease in maximal torsion. This implies that refilling an underfilled left ventricle is followed by a decrease in maximal torsion, whereas the opposite is true in normal hearts by volume challenge.[12–14]

The second interesting finding is that the peak diastolic torsion rate is elevated before closure of an atrial septal defect and returns to normal immediately after the intervention. In addition, the patients

Table 7. Patients with patent arterial ducts – demographic data.

	Patients	Control
Number	14	14*
Sex (female, male)	10, 4	10, 4*
Age (years)	2.7 ± 3.1	2.5 ± 2.5*
Weight (kg)	12.1 ± 7.2	13.1 ± 7.6*
Height (cm)	86.4 ± 25.3	86.1 ± 24.7*
BSA (m^2)	0.53 ± 0.25	0.53 ± 0.25*

BSA = body surface area
*Statistically non-significant

Table 8. Patients with PDA – standard M-mode echocardiographic measurements.

	RVDd (mm)	LVDd (mm)	LVDs (mm)	FS (%)	AoV (mm)	LA (mm)
PDA patients						
Pre	8.4 ± 2.0	35.1 ± 4.3	20.2 ± 3.7	43 ± 5	14.6 ± 2.8	25.8 ± 4.4
Post	10.4 ± 2.6	31.6 ± 4.3	19.8 ± 3.3	39 ± 6	14.2 ± 2.9	22.0 ± 4.4
	($p < 0.05$)	($p < 0.05$)	ns	($p < 0.05$)	ns	($p < 0.05$)
Control	9.4 ± 1.5	28.4 ± 7.3	15.9 ± 4.3	44 ± 5		
Pre	ns	($p < 0.05$)	($p < 0.05$)	ns		
Post	ns	ns	($p < 0.05$)	($p < 0.05$)		

AoV = aortic valve; FS = fractional shortening; LA = left atrium; LVDd = left ventricular end-diastolic diameter; LVDs = left ventricular end-systolic diameter; ns = statistically non-significant; PDA = patent arterial duct; post = after intervention; pre = before intervention; RVDd = right ventricular end-diastolic diameter
Results in mean ± SD
Differences between patient data using the paired t-test and patient and control group data compared using the unpaired t-test

Table 9. Patients with PDA – left ventricular volumetric measurements using biplanar Simpson's method.

PDA patients	LV-EDV (ml)	LV-ESV (ml)	LV-SV (ml)	CI/BSA (L/minute/m^2)	heart rate (bpm)
Pre	37.3 ± 16.8	12.5 ± 9.1	24.8 ± 9.1	5.55 ± 1.98	110 ± 27
Post	27.2 ± 10.7	10.0 ± 4.5	17.1 ± 7.1	3.67 ± 1.84	103 ± 21
	($p < 0.05$)	ns	($p < 0.05$)	($p < 0.05$)	ns

CI/BSA = cardiac index, normalised to body surface area; EDV = left ventricular end-diastolic volume; ESV = end-systolic volume; ns = statistically non-significant; PDA = patent arterial duct; post = after intervention; pre = before intervention; SV = stroke volume
Differences between patient data

https://doi.org/10.1017/S1047951113000978 Published online by Cambridge University Press

Table 10. Patients with PDA – rotational parameters.

	Tor (°/cm)	Rot_{apex} (°)	Rot_{basis} (°)	$Torrate_{sys}$ (°/second)	$Torrate_{dia}$ (°/second)
PDA patients					
Pre	1.78 ± 1.11	8.3 ± 6.1	−3.5 ± 3.9	118.4 ± 78.5	−133.2 ± 66.0
Post	2.74 ± 1.45	10.0 ± 5.7	−5.0 ± 5.0	125.8 ± 37.3	−175.6 ± 83.9
	($p < 0.05$)	ns	ns	ns	($p < 0.05$)
Control	3.80 ± 1.40	13.9 ± 4.3	−4.6 ± 2.4	161.6 ± 48.8	−158.5 ± 51.3
Pre	($p < 0.05$)	($p < 0.05$)	ns	($p = 0.091$)	ns
Post	($p = 0.059$)	($p < 0.05$)	ns	($p < 0.05$)	ns

ns = statistically non-significant; PDA = patent arterial duct; Rot_{apex} = peak systolic apical rotation; Rot_{basis} = peak systolic basal rotation; Tor = maximal torsion; $Torrate_{dia}$ = peak diastolic torsion rate; $Torrate_{sys}$ = peak systolic torsion rate; post = after intervention; pre = before intervention

Maximal and minimal values of the mean rotational curves of apical and basal short-axis loops and torsional parameters resulting from subtraction of the apical from the basal rotational curves

Results in mean ± SD

Differences between patient data using paired t-test and patient and control group data compared using the unpaired t-test

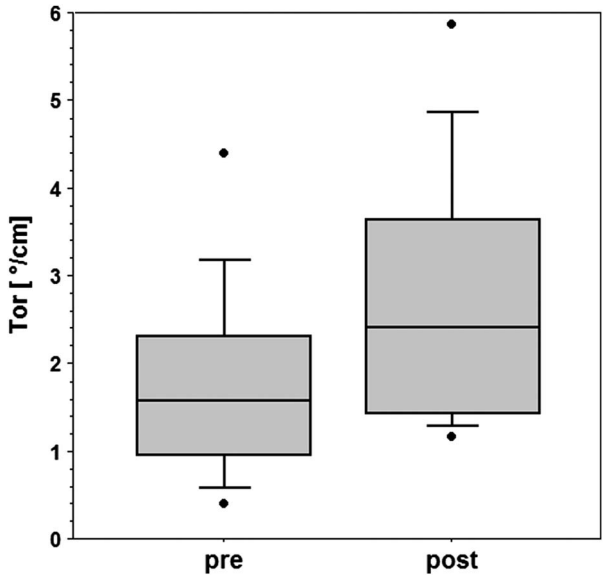

Figure 6.
Patients with patent arterial ducts – maximal torsion before and after intervention.

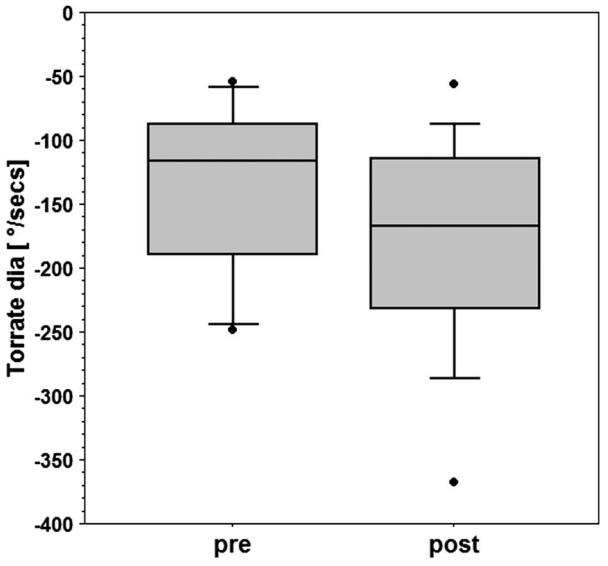

Figure 7.
Patients with patent arterial ducts – peak diastolic torsion rate before and after intervention.

in our study had increased early diastolic global longitudinal and circumferential strain rates compared with the control group. With regard to the longitudinal diastolic strain rate, this difference was no longer evident after closure of the atrial septal defects. This supports the hypothesis that enhanced diastolic filling of an elastic left ventricle in a child contributes to the maintenance of an adequate cardiac index. Another explanation could be a timing-dependent mechanism in terms of a reduced diastole because of higher heart rates before device closure and hence quicker left ventricular filling. Clinically, this could explain why children tolerate closure of atrial septal defects with less problems compared with elderly individuals who are at risk for pulmonary oedema because of left ventricular filling problems and diastolic dysfunctions.[26] It would be interesting to investigate whether the peak diastolic torsion and strain rates might be different in this setting and could help identify patients who are at higher risk for post-procedural problems.

Of the studies on left ventricular rotation after interventional shunt closure, two showed results different to those of our study. In a study population of predominantly adult patients with persistent foramen ovale and atrial septal defects,[27] cardiac magnetic resonance tagging showed a decline in basal and apical rotation after device closure,

https://doi.org/10.1017/S1047951113000978 Published online by Cambridge University Press

resulting in stable maximal torsion. Another study on adults reported an increase in maximal torsion after intervention, with improved untwisting after the procedure on speckle tracking.[28] Methodological differences in cardiac magnetic resonance imaging are a frame rate of about 20 per second in contrast to 60 per second on speckle-tracking imaging. A higher resolution might result in better detection of end-systolic and end-diastolic events. The different heart rates of patients investigated might be another important factor that may interfere with the discrepant results. In addition to methodological differences, the quantity of shunts and distensibility of the ventricles may be higher in the paediatric age group, whereas pulmonary hypertension may be higher in adult patients, resulting in right ventricular hypertrophy influencing the left ventricular/right ventricular interactions to a more intense extent. Finally, patients with a persistent foramen ovale do not have any shunt at all; this might influence the results and further undermines differences to our study.

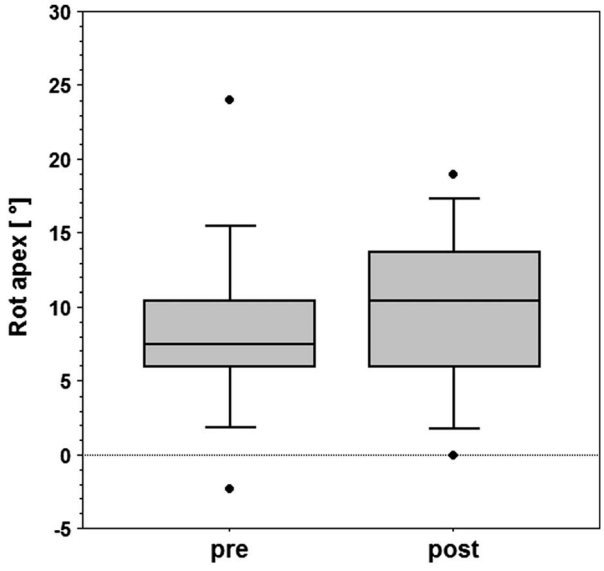

Figure 8.
Patients with patent arterial ducts – peak systolic apical rotation before and after intervention.

Patients with patent arterial ducts

Volume loading of the left ventricles in shunt lesions such as patent arterial ducts leads to a change in the shape-maintaining function and increases the output as mentioned earlier.[15] In our patients, there was a significant left ventricular dilatation that reduced to normal immediately after shunt closure. Dilatation and volume-induced hypertrophy lead to changes in muscle fibre thickness and angulations.[10] In our patients, we saw increased septal longitudinal deformations in the apical four-chamber view, especially at the mid-ventricular and apical segments. Circumferential deformations were also globally enhanced. Unlike in the atrial septal defect group, this was evident for the inferior segment, being situated opposite to the septum in the patient group. As mechanical preconditions of normal tor_{max} are important for an adequate squeezing mechanism, it can be explained why our patients with volume-loaded and balloon-shaped left ventricles had decreased maximal torsions despite hyperdynamic functions and normal ejection fractions. This can also be observed in patients with structural diseases such as dilative cardiomyopathy.[29,30] Surprisingly, maximal torsion showed a quick recompensation after interventional shunt closure, which undermines the elastic conditions of volume-dilated left ventricles at a younger age. The global and segmental longitudinal strain values decreased to normal after intervention. Although we did not observe intra-individual changes, circumferential deformations remained elevated at a segmental level and did not show significant differences after intervention when compared with the control group at a global level.

Interestingly, the peak diastolic torsion rate increased, whereas the peak early diastolic longitudinal

Table 11. Patients with PDA – global longitudinal and circumferential strain and strain rate values resulting from one apical four-chamber view including only the inter-ventricular septum and one short-axis view at the papillary muscle level before (pre) and after (post) intervention.

	GLS	GLSr	GLSr e	GLSr a	GCS	GCSr	GCSr e	GCSr a	GRS
PDA patients									
Pre	−20.71 ± 4.34	−1.49 ± 0.49	2.04 ± 0.85	1.45 ± 0.77	−21.85 ± 3.76	−1.60 ± 0.32	2.22 ± 0.76	1.15 ± 0.92	41.69 ± 19.58
Post	−16.48 ± 4.51	−1.43 ± 0.45	1.38 ± 0.59	1.47 ± 0.76	−19.37 ± 4.50	−1.55 ± 0.32	1.79 ± 0.68	1.02 ± 0.60	45.82 ± 23.72
	($p < 0.05$)	ns	($p < 0.05$)	ns	ns	ns	($p < 0.05$)	ns	ns
Control	−17.69 ± 2.83	−1.59 ± 0.42	2.43 ± 1.20	1.19 ± 0.61	−16.04 ± 3.91	−1.35 ± 0.34	1.73 ± 0.59	0.85 ± 0.53	45.49 ± 21.98
Pre	($p < 0.05$)	ns	ns	ns	($p < 0.05$)	ns	ns	ns	ns
Post	ns	ns	($p < 0.05$)	ns	($p = 0.055$)	ns	ns	ns	ns

ns = statistically non-significant; PDA = patent arterial duct
Values representing the peak systolic strain/strain rate (GLS, GCS/GLSr, GCSr) and the peak diastolic strain rate at the E-wave (GLSr e/GCSr e) and A-wave (GLSr a/GCSr a) timings

https://doi.org/10.1017/S1047951113000978 Published online by Cambridge University Press

Table 12. Patients with PDA – segmental longitudinal (GLS), radial (GRS), and circumferential (GCS) strain values resulting from one apical four-chamber view including only the interventricular septum, a basal, mid, and apical segment, and one short-axis view at the papillary muscle level including six segments (anterior, anteroseptal, inferior, lateral, posterior, and septal) before (pre) and after (post) intervention.

	Anterior	Anteroseptal	Inferior	Lateral	Posterior	Septal	Apical	Basal	Mid
PDA patients									
GCS pre	−21.04 ± 5.07	−24.23 ± 4.77	−22.46 ± 6.21	−18.59 ± 8.59	−18.63 ± 9.11	−26.31 ± 4.59			
GCS post	−17.47 ± 7.11	−21.60 ± 6.35	−21.15 ± 6.36	−16.87 ± 7.54	−19.68 ± 6.72	−23.63 ± 5.80			
	ns	ns	ns	ns	ns	ns			
GCS control	−19.96 ± 6.50	−26.13 ± 6.77	−12.05 ± 7.09	−12.21 ± 8.38	−11.52 ± 8.96	−22.43 ± 5.28			
Pre	ns	ns	($p < 0.05$)	ns	ns	ns			
Post	ns	ns	($p < 0.05$)	ns	($p < 0.05$)	ns			
GRS pre	40.20 ± 19.87	34.09 ± 15.62	44.02 ± 19.23	46.33 ± 22.21	48.77 ± 20.95	36.76 ± 18.55	40.83 ± 24.89	15.48 ± 12.47	25.51 ± 15.36
GRS post	48.20 ± 25.23	41.38 ± 15.98	44.65 ± 26.45	51.51 ± 25.19	50.18 ± 27.87	39.01 ± 21.76	28.20 ± 23.41	15.31 ± 17.59	19.27 ± 13.64
	ns	ns	ns	ns	ns	ns	ns	ns	ns
GRS control	42.09 ± 21.34	39.91 ± 23.51	49.24 ± 27.06	46.27 ± 18.64	50.39 ± 19.48	45.07 ± 23.33	45.03 ± 27.41	38.41 ± 26.80	38.76 ± 23.96
Pre	ns	ns	ns	ns	ns	ns	ns	($p < 0.05$)	ns
Post	ns	ns	ns	ns	ns	ns	ns	($p < 0.05$)	($p < 0.05$)
GLS pre							−21.14 ± 5.13	−20.23 ± 5.51	−20.73 ± 4.46
GLS post							−16.68 ± 4.86	−16.78 ± 3.99	−16.62 ± 4.35
							($p < 0.05$)	ns	($p < 0.05$)
GLS control							−17.69 ± 3.09	−17.68 ± 2.88	−17.62 ± 2.95
Pre							($p < 0.05$)	ns	($p < 0.05$)
Post							ns	ns	ns

ns = statistically non-significant; PDA = patent arterial duct
Values representing the global segmental strain

and circumferential strain rates decreased after closure of a patent arterial duct. This might be explained by a quick recompensation and improvement in diastolic filling, with a change in left ventricular morphology and regeneration of left ventricular volumes after shunt closure.

These findings are consistent with those of the study by Gupta et al,[31] who reported early recompensation of the systolic function of the left ventricle after closure of patent arterial ducts. The finding that the diastolic function regenerates later after shunt closure cannot be supported by our measurements, which were restricted to peak diastolic torsion rates and hint at earlier recompensation of diastolic dysfunction in our young patients.

The interaction between the right and left ventricles is an important and interesting field in congenital heart disease that still needs further investigation. After corrective surgery, patients with tetralogy of Fallot have limitations in right and left ventricular global strain values as well as in systolic and diastolic left ventricular rotation and torsion.[32] Further, right ventricular volume overload by significant pulmonary regurgitation has a negative correlation with left ventricular torsional mechanics.[33] In contrast, the right ventricles are not able to generate torsional mechanics even in the situation of a systemic right ventricle after Senning's procedure.[34] These aspects further hint at the importance of rotational mechanics in the development of cardiac failure in patients with congenital heart disease.

Finally, some aspects about rotational parameters in young children need further explanation. Our control groups for the patients patent arterial duct had higher values for maximal torsion, peak systolic torsion rate, peak diastolic torsion rate, and peak systolic apical rotation compared with patients with atrial septal defects. Notomi et al[19] found higher rotational values in infants and young toddlers if the values were normalised to left ventricular length. These effects might be due to the fact that heart rates are higher in smaller children and that maximal torsion correlates with the heart rate.[35] Further, there is high variability in these parameters apart from heart rates in these age groups, which is not caused by variations in reproducibility. Therefore, other confounding factors such as loading conditions might also be important. This may affirm the need for further investigations in young children, with a higher number of individuals included to generate percentiles for rotational parameters.

Limitations

Our study has some limitations that may interfere with the results presented. First, we used healthy age-matched, sex-matched, and body surface area-matched control individuals because of scarce reference values for left ventricular rotational parameters, especially for younger children. Owing to the high standard deviations in maximal torsion and the known problems of reproducibility, a higher number of patients and controls should have been investigated. In the future, the group of younger children should in particular be investigated further because they might have a more varied range of "normal" rotational values. Further, follow-up investigations of patients on functional outcome would have been interesting in order to see later changes in the deformation patterns as not all conformational changes in left ventricular mechanics might occur directly after interventional therapy. This however was not the focus of our study.

As a new generation of paediatric real-time 3D matrix probes is now available, volumetric measurements should be performed using this method for future investigations, including 3D speckle-tracking techniques.

Conclusions

Chronically volume-unloaded left ventricles in patients with right ventricular dilatation due to atrial septal defects use rotational forces to optimise filling in diastole and ejecting in systole in order to maintain an adequate cardiac index. After acute shunt closure, this is followed by a quick regeneration to normal values. In contrast, volume-overloaded left ventricles in patients with patent arterial ducts have decreased systolic rotation because of changes in the anatomical shape. These ventricles significantly improve after interventional duct closure in their systolic and diastolic performance parameters.

These results demonstrate that left ventricles of patients with congenital heart disease, shunt lesions, and, thereby, chronic volume changes show behaviours different from those of normal left ventricles under acute preload changes; this may explain the quick clinical adaptation after interventional therapy. Some of these parameters observed in this study might explain the variants of systolic and diastolic function impairment if the treatment is carried out at a later age.

Acknowledgements

None.

Conflicts of Interest

None.

References

1. Brodin LA. Tissue doppler, a fundamental tool for parametric imaging. Clin Physiol Funct Imaging 2004; 24: 147–155.

2. Van de Veire NR, De Sutter J, Bax JJ, et al. Technological advances in tissue doppler imaging echocardiography. Heart 2008; 94: 1065–1074.
3. Risum N, Ali S, Olsen NT, et al. Variability of global left ventricular deformation analysis using vendor dependent and independent two-dimensional speckle-tracking software in adults. J Am Soc Echocardiogr 2012; 25: 1195–1203.
4. Sitia S, Tomasoni L, Turiel M. Speckle tracking echocardiography: a new approach to myocardial function. World J Cardiol 2010; 2: 1–5.
5. Nakatani S. Left ventricular rotation and twist: why should we learn? J Cardiovasc Ultrasound 2011; 19: 1–6.
6. Buchalter MB, Weiss JL, Rogers WJ, et al. Noninvasive quantification of left ventricular rotational deformation in normal humans using magnetic resonance imaging myocardial tagging. Circulation 1990; 81: 1236–1244.
7. Helle-Valle T, Crosby J, Edvardsen T, et al. New noninvasive method for assessment of left ventricular rotation: speckle tracking echocardiography. Circulation 2005; 112: 3149–3156.
8. Notomi Y, Lysyansky P, Setser RM, et al. Measurement of ventricular torsion by two-dimensional ultrasound speckle tracking imaging. J Am Coll Cardiol 2005; 45: 2034–2041.
9. Notomi Y, Setser RM, Shiota T, et al. Assessment of left ventricular torsional deformation by doppler tissue imaging: validation study with tagged magnetic resonance imaging. Circulation 2005; 111: 1141–1147.
10. Buckberg G, Hoffman JIE, Nanda NC, et al. Ventricular torsion and untwisting: further insights into mechanics and timing interdependence: a viewpoint. Echocardiography 2011; 28: 782–804.
11. Dong SJ, Hees PS, Huang WM, et al. Independent effects of preload, afterload, and contractility on left ventricular torsion. Am J Physiol 1999; 277: H1053–H1060.
12. Hansen DE, Daughters GT II, Alderman EL, et al. Effect of volume loading, pressure loading, and inotropic stimulation on left ventricular torsion in humans. Circulation 1991; 83: 1315–1326.
13. Moon MR, Ingels NB Jr, Daughters GT II, et al. Alterations in left ventricular twist mechanics with inotropic stimulation and volume loading in human subjects. Circulation 1994; 89: 142–150.
14. Weiner RB, Weyman AE, Khan AM, et al. Preload dependency of left ventricular torsion: the impact of normal saline infusion. Circ Cardiovasc Imaging 2010; 3: 672–678.
15. Mathew R, Thilenius OG, Arcilla RA. Comparative response of right and left ventricles to volume overload. Am J Cardiol 1976; 38: 209–217.
16. Eerola A, Jokinen E, Boldt T, et al. The influence of percutaneous closure of patent ductus arteriosus on left ventricular size and function: a prospective study using two- and three-dimensional echocardiography and measurements of serum natriuretic peptides. J Am Coll Cardiol 2006; 47: 1060–1066.
17. Ewert P, Berger F, Nagdyman N, et al. Acute left heart failure after interventional occlusion of an atrial septal defect. Z Kardiol 2001; 90: 362–366.
18. Jeong YH, Yun TJ, Song JM, et al. Left ventricular remodeling and change of systolic function after closure of patent ductus arteriosus in adults: device and surgical closure. Am Heart J 2007; 154: 436–440.
19. Notomi Y, Srinath G, Shiota T, et al. Maturational and adaptive modulation of left ventricular torsional biomechanics: Doppler tissue imaging observation from infancy to adulthood. Circulation 2006; 113: 2534–2541.
20. Laser KT, Haas NA, Jansen N, et al. Is torsion a suitable echocardiographic parameter to detect acute changes in left ventricular afterload in children? J Am Soc Echocardiogr 2009; 22: 1121–1128.
21. Streeter D. Gross morphology and fiber geometry of the heart. In: Berne R (ed.). Handbook of Physiology. Williams and Wilkins, Baltimore, 1979: 61–112.
22. Streeter DD, Powers WE, Ross MA, et al. Three dimensional fiber orientation in the mammalian left ventricle wall. In: Baan J, Noordergraaf A, and Raines J (eds). Cardiovascular System Dynamics. MIT Press, Cambridge, MA, 1978: 73–84.
23. Torrent-Guasp F, Buckberg GD, Clemente C, et al. The structure and function of the helical heart and its buttress wrapping. I. The normal macroscopic structure of the heart. Semin Thorac Cardiovasc Surg 2001; 13: 301–319.
24. Kocica MJ, Corno AF, Carreras-Costa F, et al. The helical ventricular myocardial band: global, three-dimensional, functional architecture of the ventricular myocardium. Eur J Cardiothorac Surg 2006; 29 (Suppl 1): S21–S40.
25. Lunkenheimer PP, Redmann K, Westermann P, et al. The myocardium and its fibrous matrix working in concert as a spatially netted mesh: a critical review of the purported tertiary structure of the ventricular mass. Eur J Cardiothorac Surg 2006; 29 (Suppl 1): S41–S49.
26. Masutani S, Senzaki H. Left ventricular function in adult patients with atrial septal defect: implication for development of heart failure after transcatheter closure. J Card Fail 2011; 17: 957–963.
27. Stern H, Baurecht H, Luechinger R, et al. Does the amplatzer septal occluder device alter ventricular contraction pattern? A ventricular motion analysis by mr tagging. J Magn Reson Imaging 2012; 35: 949–956.
28. Dong L, Zhang F, Shu X, et al. Left ventricular torsional deformation in patients undergoing transcatheter closure of secundum atrial septal defect. Int J Cardiovasc Imaging 2009; 25: 479–486.
29. Jin SM, Noh CI, Bae EJ, et al. Decreased left ventricular torsion and untwisting in children with dilated cardiomyopathy. J Korean Med Sci 2007; 22: 633–640.
30. Kanzaki H, Nakatani S, Yamada N, et al. Impaired systolic torsion in dilated cardiomyopathy: reversal of apical rotation at mid-systole characterized with magnetic resonance tagging method. Basic Res Cardiol 2006; 101: 465–470.
31. Gupta SK, Krishnamoorthy K, Tharakan JA, et al. Percutaneous closure of patent ductus arteriosus in children: immediate and short-term changes in left ventricular systolic and diastolic function. Ann Pediatr Cardiol 2011; 4: 139–144.
32. van der Hulst AE, Delgado V, Holman ER, et al. Relation of left ventricular twist and global strain with right ventricular dysfunction in patients after operative "correction" of tetralogy of fallot. Am J Cardiol 2010; 106: 723–729.
33. Cheung YF, Wong SJ, Liang XC, et al. Torsional mechanics of the left ventricle in patients after surgical repair of tetralogy of fallot. Circ J 2011; 75: 1735–1741.
34. Pettersen E, Helle-Valle T, Edvardsen T, et al. Contraction pattern of the systemic right ventricle shift from longitudinal to circumferential shortening and absent global ventricular torsion. J Am Coll Cardiol 2007; 49: 2450–2456.
35. Cameli M, Ballo P, Righini FM, et al. Physiologic determinants of left ventricular systolic torsion assessed by speckle tracking echocardiography in healthy subjects. Echocardiography 2011; 28: 641–648.